Agricultural and Forest Meteorology 149 (2009) 2071–2081

Contents lists available at ScienceDirect

Agricultural and Forest Meteorology

journal homepage: www.elsevier.com/locate/agrformet

Advances in thermal infrared remote sensing for land surface modeling

William Kustas *, Martha Anderson

USDA-ARS Hydrology & Remote Sensing Lab, Beltsville, MD, USA

ARTICLE INFO

Article history:
Received 31 October 2008
Received in revised form 12 May 2009
Accepted 27 May 2009

Keywords:
Radiometric surface temperature
Energy balance
Thermal-based two-source modeling
One-source modeling
Evapotranspiration

ABSTRACT

Over 10 years ago, John Norman and co-authors proposed a thermal-based land surface modeling strategy that treated the energy exchange and kinetic temperatures of the soil and vegetated components in a unique "Two-Source Model" (TSM) approach. The TSM formulation addresses key factors affecting the convective and radiative exchange within the soil–canopy–atmosphere system, focusing on the relationship between radiometric and aerodynamic temperature. John Norman's contribution came at a time when thermal-based techniques applied to standard "One-Source Model" (OSM) for large scale land surface flux and evapotranspiration (ET) estimation were generally considered unreliable and not viable for operational remote sensing applications. Others have subsequently modified OSM schemes to accommodate the radiometric–aerodynamic temperature relationship for partial canopy cover conditions, approaching accuracies achieved with the TSM. In this study, Norman's TSM and two current OSM schemes are evaluated over a range in canopy cover and moisture conditions simulated by the Cupid model—a complex soil–vegetation–atmosphere transfer (SVAT) scheme developed by Norman that simulates the complete radiation, convection/turbulence and hydrologic processes occurring at the soil/canopy interface. The use of SVAT simulations permitted the evaluation of TSM and OSM approaches over a greater range of hydrometeorological and vegetation cover conditions than typically available from field observations. The utility of the TSM versus OSM approaches in handling extremes in moisture/vegetation cover conditions simulated by the SVAT model Cupid is presented. Generally the TSM approach outperformed the OSM schemes for the extreme conditions. Moreover, the ability of the TSM to partition ET into evaporation and transpiration components provides additional hydrologic information about the moisture status of the soil and canopy system, and about the vertical distribution of moisture in the soil profile (surface layer vs. root zone). Examples for actual landscapes are presented in the application of the TSM as incorporated within in the Atmosphere Land EXchange Inverse/Disaggregation ALEXI (ALEXI/DisALEXI) modeling system, designed for operational applications at local to continental scales using multi-scale thermal imagery. This strategy for utilizing radiometric surface temperature in land surface modeling has converted many skeptics and more importantly rejuvenated many in the research and operational remote sensing community to reconsider the utility of thermal infrared remote sensing for monitoring land surface fluxes from local to regional scales.

Published by Elsevier B.V.

1. Introduction

The partitioning of available energy at the land surface – net radiation (Rn) less the soil heat flux (G) – between sensible (H) and latent heat (LE) flux has a wide range of applications in hydrological modeling, ecosystem health assessment, weather and crop yield forecasting, drought monitoring, and in water resource management. This energy budget partitioning occurs at the leaf and canopy levels and up through regional and continental scales, with different processes controlling the partitioning at different spatial and temporal scales (Jarvis, 1993; Raupach and Finnigan, 1995).

There are numerous soil–vegetation–atmosphere transfer (SVAT) modeling approaches developed to estimate energy fluxes at the leaf and canopy levels, and others for applications at regional scales (see, e.g., review by Olioso et al., 1999). The more complex SVAT schemes, such as Cupid (Norman, 1979; Norman and Arkebauer, 1991; Norman and Campbell, 1983), explicitly model the coupled transport of radiation, heat, water and carbon through the canopy system, providing insight into the physical processes affecting soil–plant–atmosphere exchange at the canopy scale, and important feedbacks between these processes (Norman, 1993). On the other hand, detailed SVAT models are not as practical for use at landscape and regional scales because the numerous input

* Corresponding author. Tel.: +1 301 504 8498; fax: +1 301 504 8931.
E-mail address: Bill.Kustas@ars.usda.gov (W. Kustas).

0168-1923/$ – see front matter. Published by Elsevier B.V.
doi:10.1016/j.agrformet.2009.05.016

parameter fields cannot be reliably determined over large areas (Raupach and Finnigan, 1988), and because other processes (e.g., atmospheric boundary layer entrainment) are likely to govern the energy partitioning at these scales (Jarvis, 1993).

In an attempt to bridge the gap from canopy to regional scales, simpler SVAT schemes have been developed using remotely sensed data for defining important model inputs. One such category of approaches uses remotely sensed land surface temperature as a key boundary condition. Surface temperature serves as a metric for the soil moisture status and vegetation condition, which in turn influence the energy balance and partitioning of the soil–vegetation system.

The complexity of thermal-based modeling algorithms range from empirically based schemes using field data to derive relationships between energy fluxes and surface–air temperature differences, to semi-empirical methods using the surface temperature range (minimum and minimum) in the scene and energy balance constraints to define upper limit ($LE \sim \mathrm{Rn} - G$) and lower limit ($LE \sim 0$) in evaporation, and to SVAT modeling schemes that consider radiative and convective exchanges between the soil and vegetation components and the overlying atmosphere. There are a number of review articles that describe these approaches (e.g., Kustas and Norman, 1996; McVicar and Jupp, 1998; Overgaard et al., 2006). A recent and thorough review of thermal-based surface energy balance models is given by Kalma et al. (2008).

In the early 1990s, a seminal paper was published (Hall et al., 1992) that cast serious doubts about the utility of remotely sensed surface temperature for land surface modeling. This led to a response by a small but influential community of international scientists, who conducted a workshop on thermal infrared (TIR) remote sensing to review and discuss the potential of the TIR band, in conjunction with other sensor data, for estimating land surface fluxes and states (Carlson et al., 1995). Proceedings from this workshop were published in a Special Issue of Agricultural and Forest Meteorology entitled "Thermal Remote Sensing of the Energy and Water Balance over Vegetation" (Moran, 1995).

In that special issue, a paper by Norman et al. (1995) laid out a thermal-based land surface modeling strategy that explicitly treated the energy exchange and kinetic temperatures of the soil and vegetated components in a "two-source" modeling (TSM) configuration. This was inspired by earlier TSM schemes developed by Shuttleworth and Wallace (1985) and Shuttleworth and Gurney (1990) to address conditions of partial canopy cover. Norman et al. (1995) TSM scheme ($\mathrm{TSM_N}$) was specifically designed to address the key factors affecting the aerodynamic–radiometric temperature relationship that had plagued many prior applications of one-source modeling (OSM) schemes, resulting in poor performance when applied to partial canopy cover and heterogeneous landscapes unless calibrated using local observations (e.g., Kustas et al., 1996).

More recently, OSM formulations have been derived that adjust the radiometric–aerodynamic relationship based on complex physical models of the soil–canopy heat exchange (e.g., Blümel, 1999; Lhomme et al., 2000; Massman, 1999; Matsushima, 2005; Su et al., 2001). These modified OSM schemes require vegetation structure, density/leaf area, and other inputs similar to the TSM, and many can compute sensible heat flux over partial canopy cover as reliably as the TSM (e.g., Su et al., 2001). However, for the same input needs, these 'adjusted' one-source schemes provide less output information than do comparable two-source models; namely, bulk heat fluxes as opposed to fluxes partitioned between soil and canopy.

Although there have been great advances in the application of thermal infrared remote sensing for land surface flux estimation, there are still those in the research community who attempt to apply land surface temperature in OSM schemes without considering the effect of partial vegetation cover and other basic factors on the radiometric–aerodynamic temperature relationship (e.g., Cleugh et al., 2007). Such reports perpetuate unwarranted skepticism in the utility of thermal-infrared data when in fact other studies continue to show that thermal-based surface energy balance approaches have significant practical value for monitoring surface moisture and evapotranspiration at multiple spatial and temporal scales (Allen et al., 2007a,b; Anderson et al., 2007a; Hain et al., 2009; Kalma et al., 2008).

When the dependence of the aerodynamic–radiometric temperature relationship on vegetation cover fraction is properly addressed, both OSM and TSM schemes can provide good estimates of the surface energy budget partitioning (e.g., Anderson et al., 2007a; Su et al., 2001). However, most studies reported in the literature use field measurements obtained over a limited variety of land cover and hydrometeorological conditions. While model validation with field measurements is essential, it is also very useful to employ simulated data from complex SVAT models covering a wider range of moisture and vegetation cover conditions in order to gain a better understanding of how models with simplified parameterizations of soil–vegetation–atmosphere exchange perform under more extreme vegetation and environmental conditions. These more extreme cases are ones that are likely to be more difficult to reliably model and often more relevant for many agricultural and environmental applications (Moran, 2004). Therefore, in this paper, Norman's detailed Cupid SVAT model has been used to simulate land-surface temperature and fluxes for a wide range in hydrologic conditions and canopy characteristics. These simulated data are then used to evaluate a suite of OSM and TSM formulations that consider partial canopy effects, assessing their ability to reproduce Cupid-derived heat fluxes. The value of having a TSM formulation that separates the impacts of soil moisture deficiencies on soil/substrate surface evaporation and canopy transpiration will also be examined, as this is critical for agriculture (scheduling irrigation, assessing crop stress and yield) as well as natural ecosystems for evaluating plant/vegetation stress.

2. Description of OSM and TSM formulations and Cupid

2.1. The OSM formulation

The key boundary condition for many of the these models is a directional radiometric surface temperature, $T_R(\phi)$, observed at viewing angle ϕ. To simplify ϕ modeling requirements, $T_R(\phi)$ is often used to replace the so-called "aerodynamic surface temperature", which satisfies the bulk resistance formulation for sensible heat transport, H,

$$H = \rho C_P \frac{T_{OM} - T_A}{R_A} = \rho C_P \frac{T_{OH} - T_A}{R_{AH}}, \tag{1}$$

where H is the sensible heat flux (W m^{-2}), ρ is air density (kg m^{-3}), C_P is the heat capacity of air (J kg^{-1} K^{-1}), T_{OM} (K) is the aerodynamic surface temperature defined by momentum roughness (see below), T_{OH} (K) is the aerodynamic surface temperature defined by roughness for heat (see below), T_A is the air temperature in the surface layer measured at some height above the canopy (K), R_A is the aerodynamic resistance (s m^{-1}), which has the following form in the surface layer (Brutsaert, 1982):

$$R_A = \frac{[\ln((z_U - d_O)/z_{OM}) - \Psi_M][\ln((z_T - d_O)/z_{OM}) - \Psi_H]}{k^2 u}, \tag{2}$$

and $R_{AH} \equiv R_A + R_{EX}$, where R_{EX} is an excess resistance associated with heat transport (s m^{-1}) across the temperature gradient

$T_{OH} - T_A$:

$$R_{AH} = \frac{[\ln((z_U - d_O)/z_{OM}) - \Psi_M][\ln((z_T - d_O)/z_{OH}) - \Psi_H]}{k^2 u}. \quad (3)$$

In these equations d_O is the displacement height, u is the wind speed measured at height z_U, k is von Karman's constant (≈0.4), z_T is the height of the T_A measurement, Ψ_M and Ψ_H are the Monin–Obukhov stability functions for momentum and heat, respectively, and z_{OM} is the roughness length for momentum transport, and z_{OH} is the roughness length for heat transport.

The excess resistance term, R_{EX}, reflects the fact that heat must diffuse through laminar boundary layers surrounding canopy and soil elements, while momentum is transferred more efficiently as a result of viscous shear and form drag of the roughness elements involving local pressure gradients. This difference in transport mechanisms for heat and moment is often expressed as a difference in effective roughness length via Eq. (3). In resistance notation, $R_{EX} = [\ln(z_{OM}/z_{OH})]/[ku_*]$, where u_* is the friction velocity ($u_* = uk/[\ln(z_U - d_O)/z_{OM} - \Psi_M]$), and z_{OH} is typically of order $0.1z_{OM}$. When $T_R(\phi)$ is used in Eq. (1) instead of T_{OH} or T_{OM} with measured fluxes it is often found that the conceptual framework defining z_{OH} has to be revised to incorporate the so-called "radiometric roughness length" z_{OR} (e.g., Brutsaert and Sugita, 1996). This has also been represented by an additional resistance term—radiometric resistance, R_R, as illustrated in the schematic of the OSM and TSM resistance formulations (Fig. 1). However, studies evaluating z_{OR} find considerable scatter in derived values and no single formulation that clearly explains the observed variability, particularly for partial canopies (e.g., Verhoef et al., 1997).

Much effort has been expended to evaluate the behavior z_{OH}/z_{OR} for different surfaces in terms of classical boundary layer theory near roughness elements (described above). Traditionally, the efficacy of momentum versus heat transport for different surfaces is related to the ratio $\ln(z_{OM}/z_{OH}) = kB^{-1} = ku_*R_{EX}$ (Garratt and Hicks, 1973) or similarly $\ln(z_{OM}/z_{OR}) = kB_R^{-1} = ku_*R_R$ (Matsushima, 2005) using $T_R(\phi)$ observations and measurements of most of the variables in Eqs. (1)–(3). However TSM studies such as Blyth and Dolman (1995) and Lhomme et al. (1997) demonstrate that z_{OH} (and z_{OR}) depend on local surface conditions including fractional vegetation cover, soil and vegetation resistances, as well as on the available energy and humidity deficit. This is further complicated by view angle effects on the $T_R(\phi)$ observation, which in turn influences the magnitude of z_{OH} or z_{OR} (Lhomme et al., 2000). Consequently, there does not appear to be a universal methodology that can be used to derive $z_{OH}(z_{OR})$ *a priori* for all landscapes.

To accommodate the inherent differences between $T_R(\phi)$ and $T_{OM}/T_{OH}/T_{OR}$, OSMs require some means of parameterizing R_{EX}/R_R (or equivalent) in terms of observable quantities such as cover fraction. The most successful results have come from deriving formulations that adjust for differences between radiometric and aerodynamic surface temperatures based on more complex physical models of the soil–canopy heat exchange (e.g., Blümel, 1999; Lhomme et al., 2000; Massman, 1999; Matsushima, 2005; Su et al., 2001). These modified OSM schemes require vegetation structure, density/leaf area, and other inputs similar to two-source models, and can in many cases compute bulk sensible heat flux as reliably as two-source estimates over partial canopy cover (Su et al., 2001). They do not and cannot, however, provide information on how these bulk heat fluxes are partitioned between the soil and canopy. Consequently, they cannot explicitly infer canopy stress or plant water use, which is much more useful for agricultural applications and for assimilation into water balance models as a metric for root zone moisture conditions (Crow et al., 2008).

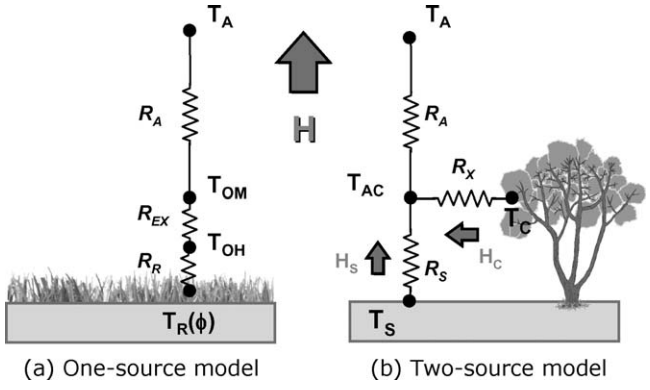

Fig. 1. Schematic of resistance network for the OSM and TSM formulations for computing sensible heat flux, H. Note that the vertical separation between temperature nodes is not to scale.

Lhomme et al. (2000) used the TSM framework originally devised by Shuttleworth and Wallace (1985) to conduct simulations under a range of vegetation cover and soil moisture conditions along with experimental data to derive and validate a relatively simple expression for estimating the B^{-1} variable. Lhomme et al. (2000) used the following expression to relate B^{-1} to the relationship between $T_R(\phi)$ and T_{OM}

$$B^{-1} = R_A u_* \frac{T_R - T_{OM}}{T_{OM} - T_A}, \quad (4)$$

Based on the TSM simulations, they found that B^{-1} could be estimated using a sixth order polynomial as a function of *LAI*. The coefficients of the polynomial were shown to vary with radiometer viewing angle, and semi-empirical expressions were given for $\phi = 0°$, $45°$ and $60°$. This modified OSM, OSM_L, was validated by Lhomme et al. (2000) using partial canopy cover data from a fallow savannah site in Niger Africa.

Matsushima (2005) developed a general parameterization to account for variability in $T_R(\phi) - T_{OH}$ based on multi-source canopy model simulations and experimental data over a rice paddy under a wide range in vegetation density conditions. Matsushima (2005) shows how z_{OR} is analytically related to the $T_R(\phi) - T_{OH}$ 'adjustment' formulations proposed originally by Chehbouni et al. (1996) and Troufleau et al. (1997). The adjustment to the one-source formulation originally proposed by Troufleau et al. (1997) is expressed by Matsushima (2005) in resistance form for his OSM scheme, OSM_M, as

$$H = \rho C_P (1 - \alpha) \frac{T_R(\phi) - T_A}{R_{AH}} \quad (5)$$

where α is defined as follows:

$$\alpha = \frac{T_R(\phi) - T_{OH}}{T_R(\phi) - T_A} \quad (6)$$

With the evaluation of Eqs. (5) and (6), using the multi-source canopy model simulations and the experimental data, Matsushima (2005) finds a relationship between α and vegetation density as quantified by *LAI*. Kustas et al. (2007) found that view angle effects had a minor impact (i.e., less than 5%) on H estimates using Eq. (5).

2.2. The TSM_N formulation

The TSM scheme originally proposed by Norman et al. (1995) has gone through several revisions, improving shortwave and longwave radiation exchange within the soil–canopy system and the soil–canopy energy exchange (Kustas and Norman, 1999a,b, 2000a,b). The current TSM formulation (TSM_N) applies only to daytime conditions, with parameterizations optimized for the

period encompassing several hours around solar noon. In the TSM_N, the satellite derived directional radiometric surface radiometric temperature, $T_R(\phi)$, is considered to be a composite of the soil and canopy temperatures, expressed as:

$$T_R(\phi) \approx [f_C(\phi)T_C^4 + (1 - f_C(\phi))T_S^4]^{1/4} \quad (7)$$

where T_C is canopy temperature, T_S is soil temperature, and $f_C(\phi)$ is the fractional vegetation cover observed at the radiometer view angle ϕ. For a canopy with a spherical leaf angle distribution and leaf area index *LAI*,

$$f_C(\phi) = 1 - \exp\left(\frac{-0.5\Omega LAI}{\cos\phi}\right) \quad (8)$$

where the factor Ω indicates the degree to which vegetation is clumped as in row crops or sparsely vegetated shrubland canopies (Kustas and Norman, 1999a, 2000b). These component temperatures are used to compute the surface energy balance for the canopy and soil components of the combined land-surface system:

$$R_{NS} = H_S + LE_S + G \quad (9)$$

$$R_{NC} = H_C + LE_C \quad (10)$$

where R_{NS} is net radiation at the soil surface and R_{NC} is net radiation divergence in the vegetated canopy layer, H_C and H_S are canopy and soil sensible heat flux, respectively, LE_C is the canopy transpiration rate, LE_S is soil evaporation, and G is the soil heat flux.

By permitting the soil and vegetated canopy fluxes to interact with each other, Norman et al. (1995) derived expressions for H_C and H_S expressed as a function of temperature differences:

with

$$H_C = \rho C_P \frac{T_C - T_{AC}}{R_X} \quad (11)$$

and

$$H_S = \rho C_P \frac{T_S - T_{AC}}{R_S} \quad (12)$$

so that the total sensible heat flux $H = H_C + H_S$ is equal to

$$H = \rho C_P \frac{T_{AC} - T_A}{R_A} \quad (13)$$

where T_{AC} is an air temperature in the canopy air layer closely related to the aerodynamic temperature T_{OM} (see Fig. 1), R_X is the total boundary layer resistance of the complete canopy of leaves, R_S is the resistance to sensible heat exchange from the soil surface and R_A is aerodynamic resistance defined by Eq. (2). The original resistance formulations are described in Norman et al. (1995) with recent revisions described in Kustas and Norman (1999a,b, 2000a,b). Weighting of the heat flux contributions from the canopy and soil components is performed indirectly by the partitioning of the net radiation between soil and canopy and via the impact on resistance values from the fractional amount and type of canopy cover (see Kustas and Norman, 1999b). The resistances R_X and R_S together with the partitioning of $T_R(\phi)$ into T_C and T_S effectively account for the excess resistance parameterizations R_{EX} and R_R in the OSM approaches, but with a more physical representation of the effect of the soil and vegetation influence on the rate of (or resistance to) turbulent heat exchange with the overlying atmosphere.

For the latent heat flux from the canopy, the Priestley–Taylor formula is used to initially estimate a potential rate for LE_C

$$LE_C = \alpha_{PTC} f_G \frac{\Delta}{\Delta + \gamma} R_{NC} \quad (14)$$

where α_{PTC} is a variable quantity related to the so-called Priestley–Taylor coefficient (Priestley and Taylor, 1972), but in this case defined exclusively for the canopy component, which was suggested for row crops by Tanner and Jury (1976). The variable α_{PTC} is normally set to an initial value ~1.3, except under well-watered partial canopy cover conditions in advective environments where a higher value ($\alpha_{PTC} \sim 2$) may be more appropriate (Castellvi et al., 2001; Kustas and Norman, 1999a), f_G is the fraction of green vegetation, Δ is the slope of the saturation vapor pressure versus temperature curve and γ is the psychrometric constant (~0.066 kPa C^{-1}). Under stress conditions, TSM_N iteratively reduces α_{PTC} from its initial value, as described below.

The latent heat flux from the soil surface is solved as a residual in the energy balance equation

$$LE_S = R_{NS} - G - H_S \quad (15)$$

with G estimated as a fraction of the net radiation at the soil surface:

$$G = c_G R_{NS} \quad (16)$$

where the value of c_G is assumed to be ~0.3 based on experimental data from several sources (Santanello and Friedl, 2003). The value of c_G varies with soil type and moisture conditions as well as time, due to the phase shift between G and R_{NS} over a diurnal cycle (Santanello and Friedl, 2003). However for the midmorning to midday period when daytime TIR satellite imagery are typically acquired, the value of c_G can be assumed constant (Kustas and Daughtry, 1990; Santanello and Friedl, 2003).

The TSM_N formulation requires both a solution to the radiative temperature balance (Eq. (7)) and the energy balance (Eqs. (9) and (10)), with physically plausible model solutions for soil and vegetation temperatures and fluxes. Non-physical solutions, such as daytime condensation at the soil surface (i.e., $LE_S < 0$), can be obtained under conditions of moisture deficiency. This happens because LE_C is overestimated in these cases by the Priestley–Taylor parameterization, which describes potential transpiration. The higher LE_C leads to a cooler T_C and T_S must be accordingly larger to satisfy Eq. (7). This drives H_S high, and the residual LE_S from Eq. (15) goes negative. If this condition is encountered by the TSM_N scheme, α_{PTC} is iteratively reduced until $LE_S \sim 0$ (expected for a dry soil surface). A more thorough discussion of conditions that force a reduction in α_{PTC}, is given by Anderson et al. (2005) and Li et al. (2005).

2.3. The Cupid model

Cupid is a detailed, multi-source SVAT model that simulates a wide variety of physiological and environmental processes simultaneously (Norman, 1979, 1988, 1993). The canopy is divided into multiple horizontal layers, and leaf density and angle distributions in each layer are prescribed. Transfer of energy, mass and momentum is assumed to occur only in the vertical dimension, and this transport is described by turbulent diffusion equations, with leaves in each layer acting as sources or sinks of various quantities. Subroutines modeling below-ground transport of heat and mass provide a description of the soil environment that surrounds the roots and incorporates the exchanges between these roots and the soil system. The Cupid model simulates all radiation, convection/turbulence and hydrologic processes occurring at the soil/canopy interface using both classical K-theory and Lagrangian

Table 1
A listing of the fluxes and radiometric surface temperature (nadir view) simulated by Cupid for the different vegetation cover, stress, surface soil moisture and wind speed conditions.

Vegetation cover	*LAI*	Vegetation condition	Soil surface	Wind ($m\ s^{-1}$)	R_N ($W\ m^{-2}$)	G ($W\ m^{-2}$)	H ($W\ m^{-2}$)	LE ($W\ m^{-2}$)	T_R (°C)
Upland shrub	0.5	Stresssed	Dry	1	457	192	226	39	55.4
	0.5	Unstressed	Dry	1	492	222	112	156	50.8
	0.5	Stressed	Dry	5	505	144	319	40	48.6
	0.5	Unstressed	Dry	5	523	175	187	160	46
Lowland shrub	1.5	Stressed	Dry	1	503	189	261	50	50.6
	1.5	Unstressed	Dry	1	563	196	40	325	42.2
	1.5	Unstressed	Wet	1	606	210	3	393	33.2
	1.5	Stressed	Dry	5	546	153	342	53	44.1
	1.5	Unstressed	Dry	5	576	172	59	345	39.8
	1.5	Unstressed	Wet	5	618	113	−32	541	30.6
Riparian shrub	3	Unstressed	Dry	1	608	122	7	476	31.7
	3	Unstressed	Wet	1	612	156	4	455	29.9
	3	Unstressed	Dry	5	618	104	−38	556	29.7
	3	Unstressed	Wet	5	624	101	−59	587	27.6
Riparian tree	3	Unstressed	Dry	1	605	124	26	448	32.5
	3	Unstressed	Wet	1	612	152	7	444	29.9
	3	Unstressed	Dry	5	610	106	48	463	31.1
	3	Unstressed	Wet	5	618	82	−17	562	28.4

methodologies (Wilson et al., 2003); however, it is a micro-meteorological model and hence does not simulate the full biogeochemical cycling of matter and nutrients, or the growth and development of vegetation.

Cupid has been tested over a wide variety of landscapes and environmental conditions (see Kustas et al., 2007 for a review). In Kustas et al. (2007, 2004), the Cupid model (K-theory version) was used to study the relationship between aerodynamic temperature, T_O, and the radiometric surface temperature, $T_R(\phi)$, incorporating directional emissivity and radiance from both vegetation and soil. Profiles of thermal radiant flux density and leaf temperature distributions are obtained in Cupid from the simultaneous solution of radiative, convective and conductive equations (Norman and Campbell, 1983). The equations approximating the radiance from each layer in the canopy and the contribution from the soil layer are described in Kustas et al. (2004) along with validation of the Cupid thermal-infrared algorithms using brightness temperature data measured in the field. For further details on how Cupid computes both convective and radiative fluxes through the soil–canopy layers see Kustas et al. (2004) and the Web site http://www.soils.wisc.edu/~norman/cupid/ where documentation and the Fortran code for running Cupid are available.

3. Description of Cupid model simulations

In this study, output is used from a set Cupid simulations of radiometric temperatures and surface fluxes for a semiarid shrubland and a riparian ecosystem under a variety of cover, moisture, and meteorological conditions This set of simulations is a subset of those used in prior validation and comparison studies reported by Kustas et al. (2004, 2007) Here, the utility of the modified OSM_M and OSM_L schemes will be compared to Cupid simulated output and contrasted to TSM_N-derived sensible heat fluxes.

Cupid was used to simulate radiometric and aerodynamic temperatures and fluxes for hypothetical semiarid shrubland/riparian sites with combinations of the following characteristics: two wind speeds (1 and 5 $m\ s^{-1}$); three vegetation cover conditions reflecting values typical of upland areas, which are usually water limited (*LAI* = 0.5), in lowland areas, typically along ephemeral channels where root zone moisture is more readily available supporting higher vegetation cover (*LAI* = 1.5), and in riparian areas where often there is ample water in the root zone to support relatively dense, taller vegetation (*LAI* = 3.0); and moisture conditions resulting in unstressed vegetation with a dry soil surface, unstressed vegetation with a moist soil surface, and stressed vegetation with a dry soil surface (see Table 1). Meteorological inputs to the model were identical at each site, typical of midday clear-sky conditions in the semiarid study area. A subset of the original simulations is used here, with solar radiation, $S = 880\ W\ m^{-2}$, vapor pressure = 1.1 kPa, and air temperature, $T_A = 28.5\ °C$. Table 1 is a summary of the different cases simulated by Cupid used in the current study (see also analyses in Kustas and Norman, 2000a; Kustas et al., 2007). As evidenced in the table, a wide range in $T_R(\phi)$ and heat fluxes is being simulated under these different soil–plant conditions. The input values describing the basic aerodynamic characteristics of the surface and variables used in the OSM and TSM schemes are listed in Table 2.

4. Comparisons of output from OSM/TSM versus Cupid

4.1. Estimates of sensible heat flux, H

A comparison of the sensible heat flux, H, simulated by Cupid versus estimates from the OSM and TSM schemes is illustrated in Fig. 2. Differences in H directly reflect how the various

Table 2
Key input variables used by OSM and TSM schemes for the four vegetation cover conditions.

Vegetation cover type	*LAI*[a]	h_C[b] (m)	z_{OM}[c] (m)	d_O[c] (m)	α_{PTC}[d]	Ω[e]
Upland shrub	0.5	0.5	0.07	0.24	2	0.7
Lowland shrub	1.5	0.5	0.045	0.36	2	0.8
Riparian shrub	3	0.5	0.03	0.39	1.5	1.0
Riparian tree	3	5	0.34	3.95	1.5	1.0

[a] *LAI*: leaf area index.
[b] h_C: canopy height with estimates based on field observations from a semiarid rangeland (Kustas and Goodrich, 1994).
[c] z_{OM} and d_O: momentum roughness length and displacement height estimated from the simplified equations of Raupach (1994) using *LAI* and h_C.
[d] α_{PTC}: Priestley–Taylor coefficient (Priestley and Taylor, 1972) used in estimating canopy transpiration in the two-source model (see Norman et al., 1995). Recently modified to be adjustable for stress and advective conditions (Kustas and Norman, 1999a; Kustas et al., 2004).
[e] Ω: clumping factor used to account for the fact that vegetation is typically clumped under sparse canopy cover conditions, thus increasing wind and radiation penetration compared to the same *LAI* randomly distributed over the surface (Kustas and Norman, 1999a,b). See also Campbell and Norman (1998).

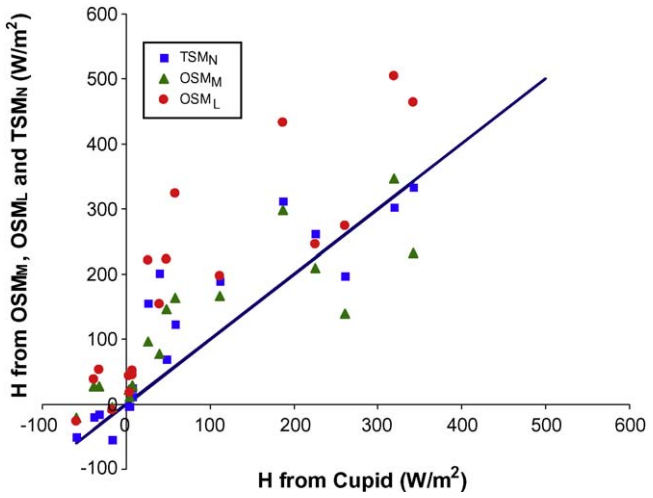

Fig. 2. Comparison of sensible heat flux H computed by Cupid versus OSM schemes of Lhomme et al. (2000), OSML, and Matsushima (2005), OSMM, and the TSM formulation of Norman et al. (1995), TSMN.

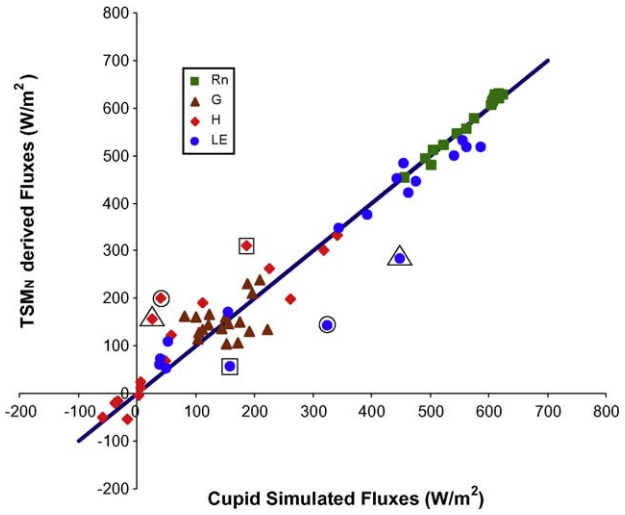

Fig. 3. Comparison of energy balance components computed by Cupid versus the TSM formulation of Norman et al. (1995), TSMN. The outliers in H and LE are for the unstressed riparian tree with a dry soil surface and wind = 1 m s^{-1} (△), the unstressed upland shrub, dry soil surface and wind = 5 m s^{-1} (□), and the unstressed lowland shrub, dry soil surface and wind = 1 m s^{-1} (○).

parameterizations define the resistances and formulations that relate the observed $T_R(\phi)$ to the aerodynamic temperature value (T_{OM} or T_{OH}) that largely defines the rate of heat flux exchange. Because the OSMs do not need to compute the full energy balance to determine a solution for H, we focus in this section on comparing the output of H from OSM_L and OSM_M with TSM_N and Cupid.

The scatter with respect to the Cupid simulations is largest with the OSM_L scheme using the B^{-1} parameterization (Eq. (4)), with a root-mean-square-difference (RMSD) of ~125 W m^{-2}. The agreement between OSM_M modified using the α formulation (Eq. (6)) and Cupid is similar to the TSM_N approach, with both yielding a RMSD of ~65 W m^{-2}. This result with OSM_M is similar to what was found by Kustas et al. (2007) in tests excluding the Cupid simulations for tall riparian vegetation.

For three of these simulated sites, TSM_N overestimates Cupid H by 100 W m^{-2}—all other sites have a RMSD value <35 W m^{-2}. A thorough analysis of the factors in TSM_N that lead to significant discrepancies with Cupid is given in the following section. The OSM schemes tend to have difficulty reproducing H for the partial canopy condition (lowland shrub case where LAI = 1.5) and stressed vegetation cases having high H. This is due in part to the fact that the adjustment/correction formulations for the radiometric–aerodynamic differences in the OSM schemes were derived for a range of environmental conditions that are not able to handle the more extreme cases simulated by Cupid.

4.2. Cupid versus TSM_N output of total and component surface energy balance

Since the TSM_N scheme requires a complete energy balance solution to compute H, all components of the energy budget were generated and can be compared to the Cupid simulated output (Fig. 3). Net radiation (R_N) is well reproduced with a RMSD of 8 W m^{-2}, while G shows larger errors (RMSD = 44 W m^{-2}). The scatter is greatest in the turbulent fluxes, H and LE, with RMSD values of ~65 and 70 W m^{-2}, respectively. This magnitude of discrepancy is somewhat higher than what has been observed when comparing both models with actual flux measurements from semiarid sites (RMSD ~ 50 W m^{-2}; Kustas et al., 2004; RMSD ~ 50 W m^{-2}; Norman et al., 1995). However, the Cupid simulations cover an extreme set of conditions often not encountered in field experiments. The outlier sites noted above are highlighted in Fig. 3—since R_N and G are reasonably reproduced, overestimates in H result in a corresponding underestimation of LE relative to the Cupid simulations.

These three cases represent the following combination of conditions: (1) the unstressed riparian tree with dry soil surface and u = 1 m s^{-1}, (2) the unstressed lowland shrub with dry soil surface and u = 1 m s^{-1}, and (3) the unstressed upland shrub with dry soil surface and u = 5 m s^{-1}. In general, the TSM_N has a tendency to overestimate H for the unstressed-vegetation dry-soil cases, where the differences between T_S and T_C are likely to be largest (Fig. 3). Looking at the relative partitioning of H and LE between the soil and canopy predicted by TSM_N and Cupid in Fig. 4, it appears that the major cause of these discrepancies is the partitioning of R_{NC} between LE_C and H_C—the soil flux components are more consistently partitioned by both models. The α_{PTC} values from TSM_N for these 3 cases are all less than 1.3, at 0.8, 0.9 and 0.8, respectively. For Cupid, the equivalent α_{PTC} values are 1.2, 1.3 and 1.5, respectively. This difference in flux partitioning for the

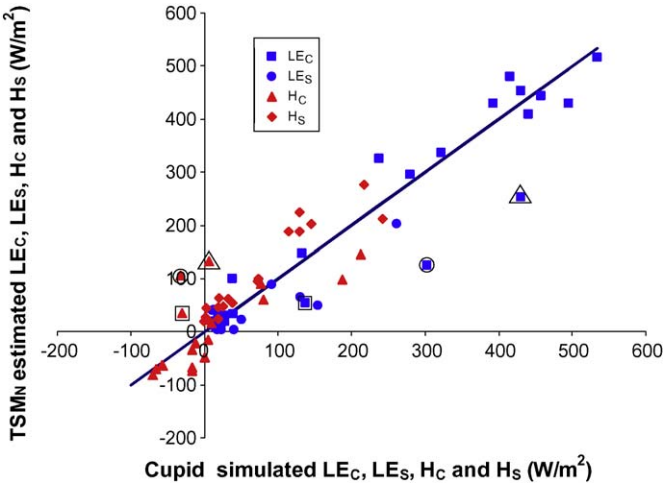

Fig. 4. Comparison of soil and canopy H and LE computed by Cupid versus the TSM formulation of Norman et al. (1995), TSMN. The outliers primarily are from differences in the partitioning of H and LE for the canopy (H_C and LE_C). The cases are the unstressed riparian tree with a dry soil surface and wind = 1 m s^{-1} (△), the unstressed upland shrub, dry soil surface and wind = 5 m s^{-1} (□), and the unstressed lowland shrub, dry soil surface and wind = 1 m s^{-1} (○).

vegetation is likely due to differences in the predicted aerodynamic resistances for the soil and canopy, particularly the low wind speed cases (u = 1 m s^{-1}), resulting in highly convective conditions where there is more uncertainty about the stability corrections and in finding a physical realistic solution (Prueger and Kustas, 2005).

Overall, however, the Priestley–Taylor α_{PTC} variable computed by the TSM$_N$ responds in an appropriate way to canopy stress and well-watered advective conditions. In the applications of TSM$_N$ described here, α_{PTC} was assigned an initial value of 2 based on the findings of Kustas and Norman (1999a) and other studies (Castellvi et al., 2001) in arid/semiarid regions, except under the high cover case (LAI = 3) where its initial value was set to 1.5 due to the likelihood that the vegetation will significantly dampen the turbulent exchange in the canopy air space (i.e., sheltering effects). An analogous quantity, α_{PTS}, can be computed for the soil by replacing in Eq. (14) R_{NC} and LE_C with $R_{NS} - G$ and LE_S:

$$\alpha_{PTS} = \frac{(\Delta/(\Delta+\gamma))(R_{NS}-G)}{LE_S} \quad (17)$$

The average and standard deviation of the α_{PTC} and α_{PTS} values computed by Cupid and the TSM$_N$ for the soil and canopy under the wet/dry soil surface and profile moisture and canopy stressed/unstressed conditions are displayed in Fig. 5. There is fairly close agreement in the average α_{PT} values from TSM and Cupid for the soil and canopy components under stressed and unstressed dry conditions, while a greater discrepancy is found for the unstressed/wet cases. In these cases, TSM$_N$ partitions more of the total LE to the canopy versus soil, in comparison with Cupid. Still, the total LE is well reproduced by TSM$_N$ for these cases. Furthermore, the exact partitioning between soil and canopy in wet conditions is not as important in many applications. However, under dry conditions, the capability of discriminating between surface soil moisture stress (affecting the soil evaporation component) and profile soil moisture stress (affecting vegetation health and functioning) is critical for many applications in agriculture, ecohydrology and assimilation of remote sensing into SVAT schemes (Crow et al., 2008).

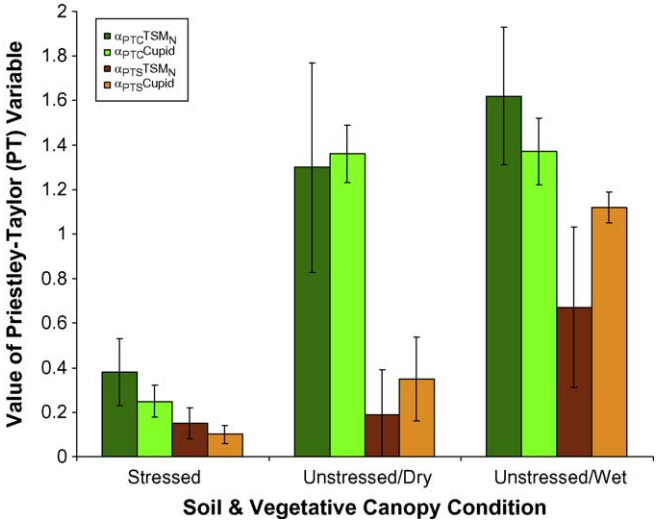

Fig. 5. Average and standard deviation of the Priestley–Taylor variable for the canopy (α_{PTC}) and the soil (α_{PTS}) from Cupid and the TSM formulation of Norman et al. (1995), TSM$_N$. The statistics for the Priestley–Taylor variables are computed for the three vegetation tress/surface soil moisture conditions, namely stressed vegetation with dry surface soil moisture (stressed), unstressed vegetation with dry surface moisture conditions (unstressed/dry), and unstressed vegetation with wet surface soil moisture conditions (unstressed/wet).

5. Applications of TSM$_N$ to actual landscapes via remote sensing

The TSM$_N$ requires land cover information similar to the OSM schemes, and since it requires no *a priori* calibration, the TSM$_N$ scheme can be applied over a range in vegetation cover conditions. It also does not require subjective intervention by a model user such as in techniques where selecting hot and cold end-members within the scene is required (e.g., Bastiaanssen et al., 1998; Allen et al., 2007a,b). By virtue of these attributes, the TSM$_N$ formulation has been successfully incorporated as the land surface modeling framework in the ALEXI/DisALEXI modeling systems designed for operational applications at local to continental scales using multi-scale TIR imagery (Anderson et al., 2007a, 1997, 2004; Mecikalski et al., 1999; Norman et al., 2003).

ALEXI/DisALEXI was designed to address the difficulty involved in accurately defining regional fields of near-surface air temperature, T_A, required in Eqs. (1) and (13) to compute the surface-to-air temperature gradient (see discussion in McVicar and Jupp, 2002; Su, 2002; McVicar et al., 2007). ALEXI circumvents the need for specifying T_A by coupling the TSM$_N$ with a simple atmospheric boundary layer (ABL) model, which internally computes T_A at the "blending height" (~50 m) rather than requiring this an input. The TSM$_N$ is applied to geostationary satellite TIR observations in a time-differencing scheme, with energy closure over a morning period of boundary layer growth provided by the ABL modeling component. This allows T_A at the blending height to respond both to local land-surface and atmospheric profile conditions. This approach can be used to automate flux predictions at the continental scale (Anderson et al., 2007a), unlike the approaches of Bastiaanssen et al. (1998) and Allen et al. (2007a,b) which require manual user intervention and assume relatively uniform meteorological conditions over the modeling domain, and are therefore better suited to targeted studies over smaller areas.

In addition, the ability of the TSM$_N$ and ALEXI/DisALEXI to separate soil and canopy fluxes provides important information concerning vegetation stress and water use under partial canopy cover conditions that is not generated in OSM schemes, even when applied successfully over the same landscape.

Benefits of the TSM$_N$ soil/canopy ET partitioning capabilities are exemplified in an application of the ALEXI/DisALEXI scheme over a corn and soybean production region in central Iowa during the 2002 Soil Moisture EXperiment/Soil Moisture Atmosphere Coupling EXperiment (SMEX02/SMACEX Kustas et al., 2005). During a period of rapid crop growth in June and July, two Landsat images (Fig. 6) were collected on June 23 2002 (day of year—DOY 174) and July 1 2002 (DOY 182). Average leaf area for soybean and corn were nominally ~1 and ~2, respectively, for DOY 174, and ~1.5 and ~3 by DOY 182. Moisture conditions varied over this time period, with a rainfall event occurring on DOY 171, wetting the soil surface in most areas with either 0–5 mm or 5–10 mm of precipitation. This was followed by a dry-down period lasting through DOY 185. As a result, although the average fractional vegetation cover increased for the study area from ~50% to 65%, there was only a marginal increase in the domain-average total LE of ~40 W m^{-2} due to the dry-down. This is consistent with the corresponding canopy transpiration and soil evaporation maps in Fig. 6. Modeled transpiration increased by 85 W m^{-2} on average across the study area, while soil evaporation decreased by 45 W m^{-2}, Accurate partitioning of LE into LE_S (soil evaporation) and LE_C (transpiration) provides valuable proxy information about the vertical distribution of moisture in the soil profile. LE_S is related to soil moisture in the upper 5–10 cm of the profile, depending on soil texture and moisture conditions (Chanzy and Bluckler, 1993; Cahill and Parlange, 1998), whereas LE_C reflects moisture conditions in the plant root zone (Anderson et al., 2007b). In turn, vertical distributions of moisture bear heavily on generating important

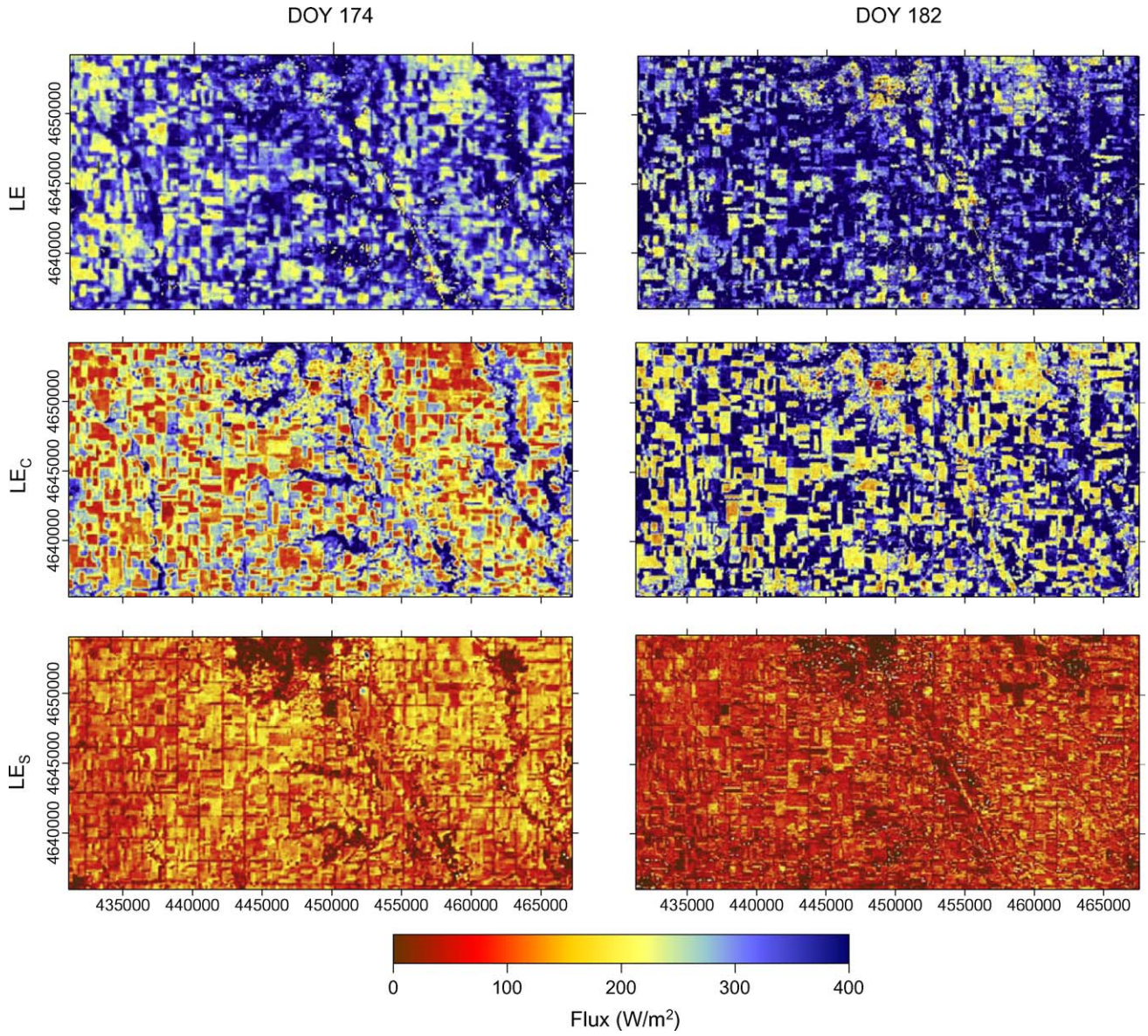

Fig. 6. Maps of canopy and soil *LE* (i.e., LE_C and LE_S, respectively) generated by ALEXI/DisALEXI over the SMEX02/SMACEX study area (see Anderson et al., 2005) during a dry down period with rapid crop (corn and soybean) growth and development. The maps are projected to UTM zone 15 coordinates (m).

hydrological fluxes, such as runoff and groundwater recharge, and effect the response of vegetation systems to droughts of various temporal extents.

Another example of soil/canopy partitioning comes from an ALEXI/DisALEXI analysis performed over the state of Oklahoma (Anderson et al., 2004). The landscapes surrounding several tower sites in the Oklahoma Mesonet (Brock et al., 1995; Brotzge and Crawford, 2003), used for validation of ALEXI/DisALEXI fluxes, were examined to see if soil and canopy contributions to *LE* provided useful information and insight to the moisture state of the surface. In Fig. 7, there are six sites displayed, ranging from high fractional vegetation cover at the top (Marena site) to low cover/bare soil dominating the scene at the bottom (Alva site). The color scale for *LE* is varied to produce optimal visual correspondence with f_C. While there is a fairly high correlation between the spatial distribution of LE_C and f_C for all sites, there is less of a direct correspondence LE_C and *LE*, particularly at low cover sites (Bessie and Alva). This is significant because it indicates that ET remote sensing models depending only on f_C or a related vegetation index (e.g., Glenn et al., 2007), may not accurately reproduce flux distributions over a full range of cover and moisture conditions. At the Bessie and Alva sites, the LST information was critical for determining spatial variability in the soil evaporation component of total ET.

Even at sites where LE_C and *LE* are well correlated in general (Marena, Stigler, Idabel, and Norman), there are areas (delineated with boxes in Fig. 6) with anomalous behavior. In these areas we find pixels with low vegetation and cool surface temperature, whereas typically T_R and f_C are anticorrelated. In each of these examples, the cool low cover areas appear to be moister than other low cover areas in the scene, either due to recent surface application/irrigation (Idabel) or shallow water tables (along the stream channel in STIG and around a small surface water body in Norman). The TSM appropriately assigns these $T_R - f_C$ anomalies to the LE_S field, as local enhancements in soil evaporation rate.

These examples show that while there are cases where ET based solely on knowledge of fractional vegetation cover could provide reasonable estimates, they require local calibration (Kalma et al., 2008) and cannot consider the effect of surface soil moisture on the *LE*. Moreover, new schemes that tout the utility of

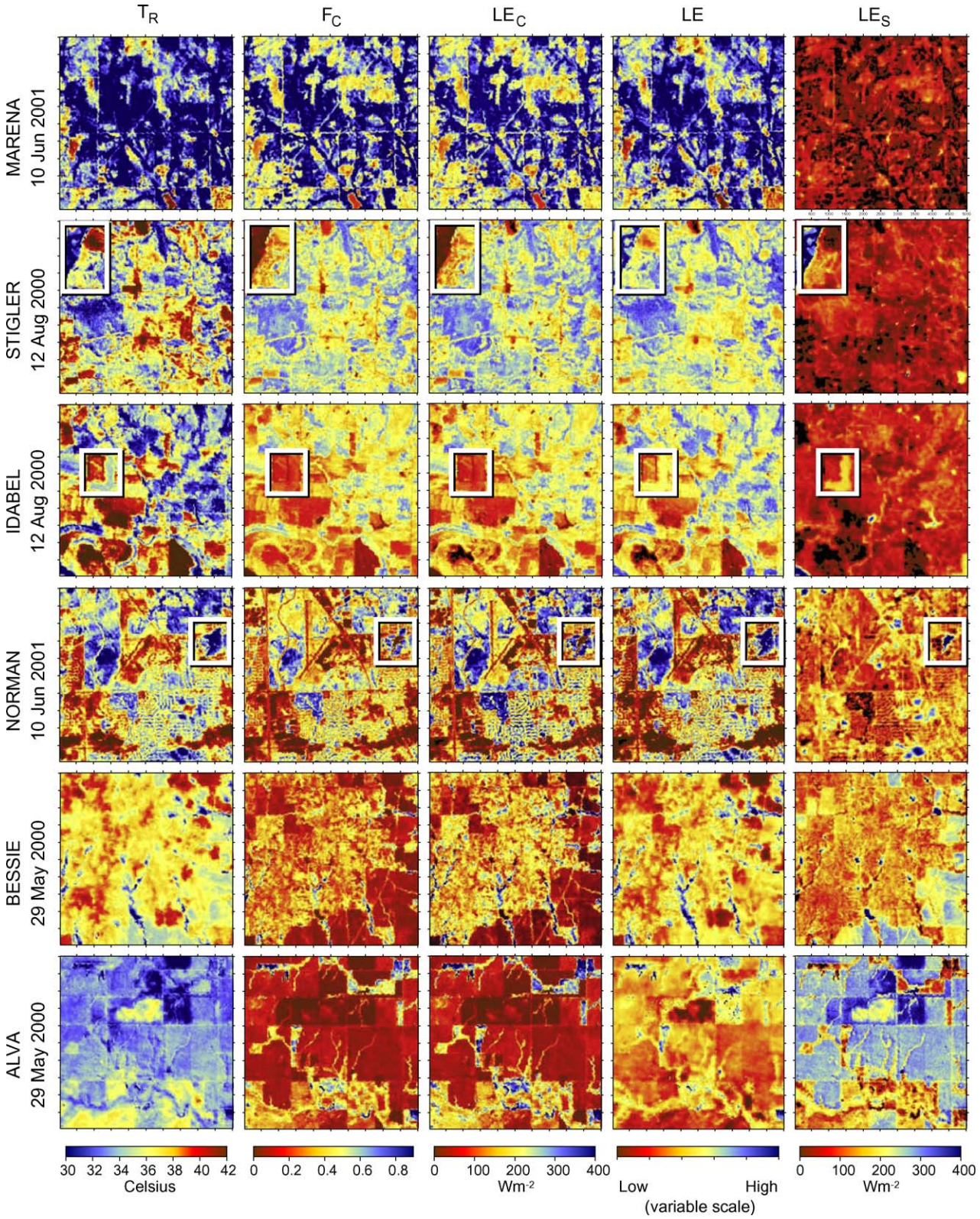

Fig. 7. Maps of radiometric surface temperature (T_R), fractional vegetation cover (f_C), and canopy *LE* (LE_C), soil *LE* (LE_S) and total *LE* ($LE_S + LE_C$) generated by ALEXI/DisALEXI for several landscapes in Oklahoma containing Mesonet flux towers (see Anderson et al., 2004). Areas delineated with boxes for the Stigler, Idabel and Norman sites show how having component *LE* fluxes can resolve anomalies in the f_C–*LE* relationship (see text). The color scale for *LE* is varied to produce optimal visual correspondence with f_C, to highlight degradation in correlation between *LE* and f_C at low cover fraction. Tick marks around grids indicate intervals of 500 m.

Penman–Monteith (e.g., Mu et al., 2007), which presumably avoids many of the pitfalls using thermal-IR, have the same issue of how they can distinguish the influence of surface moisture on *LE* without local precipitation and other weather information or training of the conductance formulation. This is a major drawback of many SVAT-based water balance models that rely critically on precipitation and other local input, which has significant spatial and temporal uncertainty. This has sparked a keen interest into

assimilation of radiometric temperature and/or thermal-based model output that can act as a soil moisture proxy and used to constrain SVAT model predictions (Crow et al., 2008; Hain et al., 2009; Renzullo et al., 2008).

6. Concluding remarks

John Norman's contribution came at a time when thermal-based techniques for large scale land surface flux and evapotranspiration (ET) estimation were generally considered unreliable and not viable for operational remote sensing applications. However, his new paradigm of how to utilize radiometric surface temperature in land surface modeling has converted many skeptics and more importantly rejuvenated many in the research and operational remote sensing community to reconsider the utility of thermal infrared remote sensing for monitoring land surface fluxes from local to regional scales (Diak et al., 2004).

The impact of John Norman's TSM formulation continues to expand the use of remotely sensed surface temperature into a number of important research and applications areas. These include investigating the role of landscape variability in surface-atmosphere feedbacks and atmospheric boundary layer dynamics via incorporation of the TSM formulation into a Large Eddy Simulation model (e.g., Albertson et al., 2001; Bertoldi et al., 2008; Kustas and Albertson, 2003), evaluating the errors in heat flux estimation by sharpening coarse resolution thermal-infrared data to sub-field scale (Agam et al., 2008), assessing the utility of assimilating radiometric surface temperature by variational approaches for heat flux partitioning and heat transfer coefficient retrieval (Crow and Kustas, 2005), exploring the utility of assimilation of a thermal-based soil moisture proxy derived from the TSM scheme (Crow et al., 2008), and development of a thermal-based multi-scale scale ET and physically based drought monitoring system being applied over the continental U.S. (Anderson et al., 2007b,c).

Although there are numerous examples supporting the use of thermal-infrared for a wide variety of applications in hydrological modeling, ecosystem health assessment, weather forecasting and crop water use and yield, others continue to claim that it has no potential for regional ET applications (e.g., Cleugh et al., 2007). However, these claims are often derived from studies using non-optimal or outdated thermal modeling techniques and do not reflect advancements made over the past decade. Such statements serve to undermine development of new thermal-based remote sensing tools and satellite imaging systems that have shown to be valuable for addressing critical questions in water resource management (Kalma et al., 2008; Anderson and Kustas, 2008).

References

Agam, N., Kustas, W.P., Anderson, M.C., Li, F., Colaizzi, P.D., 2008. Utility of thermal image sharpening for monitoring field-scale evapotranspiration over rainfed and irrigated agricultural regions. J. Geophys. Res. Lett. 35 , doi:10.1029/2007GL032195.

Albertson, J.D., Kustas, W.P., Scanlon, T.M., 2001. Large-eddy simulation over heterogeneous terrain with remotely sensed land surface conditions. Water Resour. Res. 37, 1939–1953.

Allen, R.G., Tasumi, M., Trezza, R., 2007a. Satellite-based energy balance for Mapping Evapotranspiration with Internalized Calibration (METRIC)-Model. J. Irrig. Drainage Eng. 133 (4), 380–394.

Allen, R.G., Tasumi, M., Morse, A., Trezza, R., Wright, J.L., Bastiaanssen, W., Kramber, W., Lorite, I., Robison, C.W., 2007b. Satellite-based energy balance for Mapping Evapotranspiration with Internalized Calibration (METRIC)-Applications. J. Irrig. Drain. Eng. 133 (4), 395–406.

Anderson, M.C., Kustas, W.P., 2008. Thermal remote sensing of drought and evapotranspiration. Eos, Trans. AGU 89, 233–234.

Anderson, M.C., Kustas, W.P., Norman, J.M., 2007a. Upscaling flux observations from local to continental scales using thermal remote sensing. Agron. J. 99, 240–254.

Anderson, M.C., Norman, J.M., Diak, G.R., Kustas, W.P., Mecikalski, J.R., 1997. A two-source time-integrated model for estimating surface fluxes using thermal infrared remote sensing. Remote Sens. Environ. 60, 195–216.

Anderson, M.C., Norman, J.M., Kustas, W.P., Li, F., Prueger, J.H., Mecikalski, J.R., et al., 2005. Effects of vegetation clumping on two-source model estimates of surface energy fluxes from an agricultural landscape during SMACEX. J. Hydrometeorol. 6, 892–909.

Anderson, M.C., Norman, J.M., Mecikalski, J.R., Otkin, J.P., Kustas, W.P., 2007b. A climatological study of evapotranspiration and moisture stress across the continental U.S. based on thermal remote sensing: I. Model formulation. J. Geophys. Res. 112, D10117, doi:10.1029/2006JD007506.

Anderson, M.C., Norman, J.M., Mecikalski, J.R., Otkin, J.P., Kustas, W.P., 2007c. A climatological study of evapotranspiration and moisture stress across the continental U.S. based on thermal remote sensing: II. Surface moisture climatology. J. Geophys. Res. 112, D11112, doi:10.1029/2006JD007507.

Anderson, M.C., Norman, J.N., Mecikalski, J.R., Torn, R.D., Kustas, W.P., Basara, J.B., et al., 2004. A multi-scale remote sensing model for disaggregating regional fluxes to micrometeorological scales. J. Hydrometeorol. 5, 343–363.

Bastiaanssen, W.G.M., Menenti, M., Feddes, R.A., Holtslag, A.A.M., 1998. A remote sensing surface energy balance algorithm for land (SEBAL). 1. Formulation. J. Hydrol. 212–213, 198–212.

Bertoldi, G., Kustas, W.P., Albertson, J.D., 2008. Estimating spatial variability in atmospheric properties over remotely sensed land-surface conditions. J. Appl. Meteorol. 47, 2147–2165.

Blümel, K., 1999. A simple formula for estimation of the roughness length for heat transfer over partly vegetated surfaces. J. Appl. Meteorol. 38, 814–829.

Blyth, E.M., Dolman, A.J., 1995. The roughness length for heat of sparse vegetation. J. Appl. Meteorol. 34, 583–585.

Brock, F.V., Crawford, K.C., Elliott, R.L., Cuperus, G.W., Stadler, S.J., Johnson, H.L., Eilts, M.D., 1995. The Oklahoma Mesonet: a technical overview. J. Atmos. Oceanic Technol. 12, 5–19.

Brotzge, J.A., Crawford, K.C., 2003. Examination of the surface energy budget: a comparison of eddy correlation and Bowen ratio measurement systems. J. Hydrometeorol. 4, 160–178.

Brutsaert, W., 1982. Evaporation into the Atmosphere: Theory, History and Applications. D. Reidel, Dordrecht, Holland, 299 pp.

Brutsaert, W., Sugita, M., 1996. Sensible heat transfer parameterization for surfaces with anisothermal dense vegetation. J. Atmos. Sci. 53, 209–216.

Cahill, A.T., Parlange, M.B., 1998. On water vapor transport in field soils. Water Resour. Res. 34, 731–739.

Chanzy, A., Bluckler, L., 1993. Significance of soil surface moisture with respect to daily bare soil evaporation. Water Resour. Res. 29, 1113–1125.

Campbell, G.S., Norman, J.M., 1998. An Introduction to Environmental Biophysics. Springer-Verlag, New York.

Carlson, T.N., Gillies, R.R., Schmugge, T.J., 1995. An interpretation of methodologies for indirect measurement of soil water content. Agric. For. Meteorol. 77, 191–205.

Castellvi, F., Stockle, C.O., Perez, P.J., Ibanez, M., 2001. Comparison of methods for applying the Priestley–Taylor equation at a regional scale. Hydrol. Process. 15, 1609–1620.

Chehbouni, A., Lo Seen, D., Njoku, E.G., Monteny, B., 1996. Examination of the difference between radiometric and aerodynamic surface temperatures over sparsely vegetated surfaces. Remote Sens. Environ. 58, 177–186.

Cleugh, H.A., Leuning, R., Mu, G., Running, S.W., 2007. Regional evaporation estimates from flux tower and MODIS satellite data. Remote Sens. Environ. 106, 285–304.

Crow, W.T., Kustas, W.P., 2005. Utility of assimilating surface radiometric temperature observations for evaporative fraction and heat transfer coefficient retrieval. Boundary-Layer Meteorol. 115, 105–130.

Crow, W.T., Kustas, W.P., Prueger, J.H., 2008. Monitoring root-zone soil moisture through the assimilation of a thermal remote sensing-based soil moisture proxy into a water balance model. Remote Sens. Environ. 112, 1268–1281.

Diak, G.R., Mecikalski, J.R., Anderson, M.C., Norman, J.M., Kustas, W.P., Torn, R.D., DeWolf, R.L., 2004. Estimating land-surface energy budgets from space: review and current efforts at the University of Wisconsin–Madison and USDA-ARS. Bull. Am. Meteorol. Soc. 85, 65–78.

Garratt, J.G., Hicks, B.B., 1973. Momentum, heat and water vapor transfer to and from natural and artificial surfaces. Q. J. R. Meteorol. Soc. 99, 680–687.

Glenn, E.P., Huete, A.R., Nagler, P.L., Hirschboeck, K.K., Brown, P., 2007. Integrating remote sensing and ground methods to estimate evapotranspiration. Crit. Rev. Plant Sci. 26, 139–168.

Hain, C.R., Mecikalski, J.R., Anderson, M.C., 2009. Retrieval of an available water-based soil moisture proxy from thermal infrared remote sensing. Part I: methodology and validation. doi:10.1175/2008JHM1024.1, in press.

Hall, F.G., Huemmrich, K.F., Goetz, S.J., Sellers, P.J., Nickerson, J.E., 1992. Satellite remote sensing of surface energy balance: success, failures and unresolved issues in FIFE. J. Geophys. Res. 97, 19,061–19,089.

Jarvis, P.G., 1993. Prospects for bottom-up models. In: Ehleringer, J.R., Field, C.B. (Eds.), Scaling Physiological Processes Leaf to Globe. Academic Press, San Diego, pp. 115–126.

Kalma, J.D., McVicar, T.R., McCabe, M.F., 2008. Estimating land surface evaporation: a review of methods using remotely sensing surface temperature data. Surv. Geophys., doi:10.1007/s10712-008-9037-z.

Kustas, W.P., Albertson, J.D., 2003. Effects of surface temperature contrast on land-atmosphere exchange: a case study from Monsoon 90. Water Resour. Res. 39 , doi:10.1029/2001WR001226.

Kustas, W.P., Anderson, M.C., Norman, J.M., Li, F., 2007. Utility of radiometric–aerodynamic temperature relations for heat flux estimation. Boundary-Layer Meteorol. 122, 167–187.

Kustas, W.P., Daughtry, C.S.T., 1990. Estimation of the soil heat flux/net radiation ratio from spectral data. Agric. For. Meteorol. 49, 205–223.
Kustas, W.P., Goodrich, D.C., 1994. Preface, MONSOON'90 multidisciplinary experiment. Water Resour. Res. 30, 1211–1225.
Kustas, W.P., Hatfield, J.L., Prueger, J.H., 2005. The Soil Moisture-Atmosphere Coupling Experiment (SMACEX): Background, hydrometeorological conditions, and preliminary findings. J. Hydromet. 6, 791–804.
Kustas, W.P., Humes, K.S., Norman, J.M., Moran, M.S., 1996. Single- and dual-source modeling of surface energy fluxes with radiometric surface temperature. J. Appl. Meteorol. 35, 110–121.
Kustas, W.P., Norman, J.M., 1996. Use of remote sensing for evapotranspiration monitoring over land surfaces. Hydrol. Sci. J. 41, 495–516.
Kustas, W.P., Norman, J.M., 1999a. Evaluation of soil and vegetation heat flux predictions using a simple two-source model with radiometric temperatures for partial canopy cover. Agric. For. Meteorol. 94, 13–29.
Kustas, W.P., Norman, J.M., 1999b. Reply to comments about the basic equations of dual-source vegetation-atmosphere transfer models. Agric. For. Meteorol. 94, 275–278.
Kustas, W.P., Norman, J.M., 2000a. Evaluating the effects of subpixel heterogeneity on pixel average fluxes. Remote Sens. Environ. 74, 327–342.
Kustas, W.P., Norman, J.M., 2000b. A two-source energy balance approach using directional radiometric temperature observations for sparse canopy covered surfaces. Agron. J. 92, 847–854.
Kustas, W.P., Norman, J.M., Schmugge, T.J., Anderson, M.C., 2004. Mapping surface energy fluxes with radiometric temperature. In: Quattrochi, D.A., Luvall, J.C. (Eds.), Thermal Remote Sensing in Land Surface Processes. CRC Press, Boca Raton, FL, pp. 205–253.
Lhomme, J.P., Chehbouni, A., Monteny, B., 2000. Sensible heat flux-radiometric surface temperature relationship over sparse vegetation: parameterizing B-1. Boundary-Layer Meteorol. 97, 431–457.
Lhomme, J.P., Troufleau, D., Monteny, B., Chehbouni, A., Baudin, S., 1997. Sensible heat flux and radiometric surface temperature over sparse Sahelian vegetation II: a model for the kB-1 parameter. J. Hydrol. 188–189, 839–854.
Li, F., Kustas, W.P., Prueger, J.H., Neale, C.M.U., Jackson, T.J., 2005. Utility of remote sensing based two-source energy balance model under low and high vegetation cover conditions. J. Hydrometeorol. 6, 878–891.
Massman, W., 1999. A model study of kBH-1 for vegetated surfaces using 'localized near-field Lagrangian' theory. J. Hydrol. 223, 27–43.
Matsushima, D., 2005. Relations between aerodynamic parameters of heat transfer and thermal-infrared thermometry in the bulk surface formulation. J. Meteorol. Soc. Jpn. 83, 373–389.
McVicar, T.R., Jupp, D.L.B., 1998. The current and potential operational uses of remote sensing to aid decisions on Drought Exceptional Circumstances in Australia: a review. Agric. Syst. 57, 399–468.
McVicar, T.R., Jupp, D.L.B., 2002. Using covariates to spatially interpolate moisture availability in the Murray-Darling Basin: a novel use of remotely sensed data. Remote Sens. Environ. 79, 199–212.
McVicar, T.R., Van Niel, T.G., Li, L.T., Hutchinson, M.F., Mu, X.M., Liu, Z.H., 2007. Spatially distributing monthly reference evapotranspiration and pan evaporation considering topographic influences. J. Hydrol. 338, 196–220.
Mecikalski, J.M., Diak, G.R., Anderson, M.C., Norman, J.M., 1999. Estimating fluxes on continental scales using remotely-sensed data in an atmosphere–land exchange model. J. Appl. Meteorol. 38, 1352–1369.
Moran, M.S., 1995. Thermal remote sensing. Agric. For. Meteorol. 77, v–vii.
Moran, M.S., 2004. Thermal infrared measurement as an indicator of plant ecosystem health. In: Quattrochi, D.A., Luvall, J.C. (Eds.), Thermal Remote Sensing in Land Surface Processes. CRC Press, Boca Raton, FL, pp. 257–282.
Mu, Q., Heinsch, F.A., Zhao, M.S., Running, S.W., 2007. Development of a global evapotranspiration algorithm based on MODIS and global meteorology data. Remote Sens. Environ. 111, 519–536.
Norman, J.M., 1979. Modeling the complete crop canopy. In: Barfield, B.J., Gerber, J.F. (Eds.), Modification of the Aerial Environment of Plants. Am. Soc. Agric. Eng., St. Joseph, MI, pp. 249–277
Norman J.M., 1988. Synthesis of canopy processes. In: Russell G. et al. (eds) plant canopies: their growth, form and function, Soc. Exp. Biol, Seminar Series 31, Cambridge University Press, New York, pp 161–175.
Norman, J.M., 1993. Scaling Processes Between Leaf and Canopy Levels, Scaling Physiological Processes: Leaf to Globe. Academic Press, pp. 41–76.
Norman, J.M., Anderson, M.C., Kustas, W.P., French, A.N., Mecikalski, J.R., Torn, R.D., Diak, G.R., Schmugge, T.J., Tanner, B.C.W., 2003. Remote sensing of surface energy fluxes at 10^1-m pixel resolutions. Water Resour. Res. 39 , doi:10.1029/2002WR001775.
Norman, J.M., Arkebauer, T.J., 1991. Predicting Canopy Photosynthesis and Light-use Efficiency from Leaf Characteristics, Modeling Crop Photosynthesis—From Biochemistry to Canopy, CSSA Special Publication No. 19. ASA–CSSA, Madison, pp. 75–94.
Norman, J.M., Campbell, G., 1983. Application of a plant–environment model to problems in irrigation. In: Hillel, D. (Ed.), Advances in Irrigation. Academic Press, New York, pp. 156–188.
Norman, J.M., Kustas, W.P., Humes, K.S., 1995. A two-source approach for estimating soil and vegetation energy fluxes from observations of directional radiometric surface temperature. Agric. For. Meteorol. 77, 263–293.
Olioso, A., Chauki, H., Couralt, D., Wigneron, J.-P., 1999. Estimation of evapotranspiration and photosynthesis by assimilation of remote sensing data into SVAT models. Remote Sens. Environ. 68, 341–356.
Overgaard, J., Rosbjerg, D., Butts, M.B., 2006. Land-surface modelling in hydrological perspective—a review. Biogeoscience 3, 229–241.
Priestley, C.H.B., Taylor, R.J., 1972. On the assessment of surface heat flux and evaporation using large-scale parameters. Mon. Weather Rev. 100, 81–92.
Prueger, J.H., Kustas, W.P., 2005. Aerodynamic methods for estimating turbulent fluxes. In: Hatfield, J.L., Baker, J.L. (Eds.), Micrometeorology in Agricultural Systems, Agronomy Monograph No. 47. ASA–CSSA–SSSA, Madison, WI, pp. 407–436.
Raupach, M.R., 1994. Simplified expressions for vegetation roughness length and zero-plane displacement as functions of canopy height and area index. Boundary-Layer Meteorol. 71, 211–216 (Corrigenda 76, 303–304).
Raupach, M.R., Finnigan, J.J., 1988. Single layer models of evaporation from plant canopies are incorrect, but useful, whereas multilayer models are correct, but useless: discussion. Aust. J. Plant Physiol. 15, 705–716.
Raupach, M.R., Finnigan, J.J., 1995. Scale issues in boundary-layer meteorology: surface energy balances in heterogeneous terrain. Hydrol. Process. 9, 589–612.
Renzullo, L.J., Barrett, D.J., Marks, A.S., Hill, M.J., Guerschman, J.P., Mu, Q., 2008. Multi-sensor model-data fusion for estimation of hydrologic and energy flux parameters. Remote Sens. Environ. 112, 1306–1319.
Santanello, J.A., Friedl, M.A., 2003. Diurnal variation in soil heat flux and net radiation. J. Appl. Meteorol. 42, 851–862.
Shuttleworth, W.J., Gurney, R.J., 1990. The theoretical relationship between foliage temperature and canopy resistance in sparse crop. Q. J. R. Meteorol. Soc. 116, 497–519.
Shuttleworth, W.J., Wallace, J.S., 1985. Evaporation from sparse crops—an energy combination theory. Q. J. R. Meteorol. Soc. 111, 839–855.
Su, Z., 2002. The Surface Energy Balance System (SEBS) for estimation of turbulent heat fluxes. Hydrol. Earth Syst. Sci. 6, 85–99.
Su, Z., Schmugge, T.J., Kustas, W.P., Massman, W.J., 2001. An evaluation of two models for estimation of the roughness height for heat transfer between the land surface and the atmosphere. J. Appl. Meteorol. 40, 1933–1951.
Tanner, C.B., Jury, W.A., 1976. Estimating evaporation and transpiration from a row crop during incomplete cover. Agron. J. 68, 239–242.
Troufleau, D., Lhomme, J.P., Monteny, B., Vidal, A., 1997. Sensible heat flux and radiometric surface temperature over sparse Sahelian vegetation. I. An experimental analysis of the kB-1 parameter. J. Hydrol. 188–189, 815–838.
Verhoef, A., De Bruin, H.A.R., van den Hurk, B.J.J.M., 1997. Some practical notes on the parameter kB^{-1} for sparse vegetation. J. Appl. Meteorol. 36, 560–572.
Wilson, T.B., Norman, J.M., Bland, W.L., Kucharik, C.J., 2003. Evaluation of the importance of 'lagrangian' canopy turbulence formulations in a soil–plant–atmosphere model. Agric. For. Meteorol. 115, 51–69.